Slag entraining vortexing funnel formation during ladle teeming: Similarity criteria and scale-up relationships

Ramani Sankaranarayanan[1] and Roderick I.L. Guthrie[2]

[1]HATCH
2800 Speakman Drive,
Mississauga, Ontario, Canada L5K 2R7

[2]McGill Metals Processing Centre
McGill University, 3610 University Street
Montreal, Quebec, Canada H3A 2B2

ABSTRACT

There are several motivations for minimising slag entrainment during the teeming of steelmaking ladles. Cleaner steel, improved yield and higher productivity are all at stake. As one of several identifiable contributors to slag entrainment, vortexing has received considerable attention in the past decade and a half. What is commonly referred to as "**vortexing**" in fact comprises two distinct phenomena, *viz*., **vortexing funnels** and **non-vortexing funnels**, each controlled by entirely different sets of variables.

Dimensionless relationships for the critical heights for the formation of non-vortexing funnels and vortexing funnels, $H_{cr,nvf}$ and $H_{cr,vf}$, respectively, are compared and contrasted in this paper. The principles of dimensional analysis are used to show that while $H_{cr,nvf}/d$ is related to $Q_{cr,nvf}/(g' d^5)^{0.5}$, $H_{cr,vf}/H_i$ is controlled by the vortex number, $(V_{\theta,i}\ D)/(V_{out,i}\ d)$, where d and D represent the diameters of the nozzle and ladle respectively, $Q_{cr,nvf}$ is the critical flow rate at the onset of non-vortexing funnel flow; H_i, $V_{out,i}$ and $V_{\theta,i}$ represent the initial height of liquid, the initial outflow velocity and the initial tangential velocity at the start of ladle teeming, respectively; and g' stands for $g(1 - \rho_2/\rho_1)$ where g is the acceleration due to gravity and ρ_2 and ρ_1 represent the densities of the lighter and heavier fluids (slag and steel, oil and water, or air and water), respectively. Dimensional analyses are supported with experimental evidence from aqueous (water as well as water-oil) models of steelmaking ladles. Froude number based similarity criteria, physical properties of slag (oil) and steel (water), and scale-up considerations are discussed. Performance results of a "*vortex buster*" device, designed to suppress slag entrainment on the basis of the above-mentioned correlations, are also presented from water model and plant trials.

---

[1] formerly Research Associate, McGill Metals Processing Centre, at the time the experiments were carried out.

1. Introduction

It is well established that slags in the steelmaking furnace, ladle, tundish and mould can, and do, act as sources of exogenous oxide inclusions in continuously cast steel.[1,2] Steel cleanness levels have continued to improve over the last twenty years, thanks to concerted efforts in the industry to improve product quality through a better understanding of the physical and chemical phenomena involved. Various clean steel practices have already helped eliminate/minimize many sources and types of deleterious inclusions. More exacting cleanness controls must no doubt be developed to meet further challenges in the coming years.

In work by Cramb and Byrne reporting on the entrainment of tundish slag, BaO and CeO_2 were added to the ladle and tundish slags, respectively, in order to identify them uniquely.[1,2] The slag tracers were added at the end of BOF tapping into the ladle. Samples of tundish and mold slags, and of continuously cast slab, were taken throughout a two-ladle sequence during which the ladle shroud had been kept in place throughout teeming. Inclusions obtained prior to, and up to four minutes after, the ladle change did not contain any Ba or Ce tracers, indicating that they must have been created prior to the tracer addition, *i.e.*, during BOF tapping itself. The teeming of the first ladle was ended only after significant amounts of ladle slag carryover into the tundish had occurred. Ba was the first to show up in the mould slag. The fact that Ba alone reported to the mould slag, without any Ce, from about 4 minutes after ladle change to 8 minutes after, can be explained in terms of an entrained slag funnel in the ladle having broken up into fine droplets as it passed through the nozzle into the ladle shroud; some of the smaller micro-droplets should have stayed entrained in the steel as it flowed through the tundish into the mould. Even though Cramb and Byrne did not make this connection, similar breaking up of oil (slag) entrained via vortexing, as well as non-vortexing funnels, was observed in water modelling experiments in the current authors' laboratories.[3] Larger ladle slag droplets carried into the tundish with the slag funnel, immediately prior to the end of teeming of the first ladle, no doubt floated out to the tundish slag's surface, and became well-mixed in the tundish slag. Naturally, the emulsification of the tundish slag in the pouring box during the initial stages of teeming of the second ladle, and its distribution throughout the tundish, contributed to Ba and Ce being detected together in the mould slag after the elapse of 8 minutes after the ladle change;[1,2] Ba and Ce concentrations in the mould slag peaked about 12 minutes later, and proceeded to decline steadily until the end of the second heat. Byrne, Cramb and Fenicle[1] also reported that both Ba and Ce occurred together in inclusions found in steel slab samples taken following the ladle change. Jacobi and Wünnenberg[4] also identified ladle slag drainage into the tundish as a source of oxide inclusions in cast steel.

Having said that, it is also true that very little *hard* evidence is available in the published literature about the respective contributions of slag entrainment via vortexing *versus* non-vortexing funnel formation to the overall inclusion content of cast and rolled steel products.

Given that vortexing funnel formation requires residual tangential motion to be present at the start of ladle teeming, the propensity to form vortexing funnels either may not exist at all, or it may vary from heat to heat, day to day, and from plant to plant. Several known sources of adventitious rotation do exist, including furnace tapping, argon and induction stirring, ladle transportation, rotation on the turret, *etc*. Evidently, the net residual rotation will be a complex function of interactions between successive inertial movements and time lags separating them.

However, non-vortexing funnel induced slag entrainment will inevitably occur towards the end of teeming every heat, so long as the slide gate is not closed in time. Hence the proliferation in the number of commercially available *slag sensors* and *slag-cut* devices.

Steelmakers' interests in slag sensors are manifold. Without reliable automated sensors, the operator must have visual access to the ladle stream, necessitating open pouring for up to five minutes in back-to-back heats. Even more harmful than the reoxidation of the steel during open pouring, the open stream leads to severe tundish slag emulsification and distribution throughout the tundish. Steel cleanness levels are known to drop instantaneously, once the ladle shroud is no longer present or even when it is no longer submerged. It typically requires more than 10 to 15 minutes, following the re-immersion of the ladle shroud, for steel cleanness levels to recover to those prevalent prior to the open pouring event. Operator error and skill variability represent factors affecting yield and consistency of operation. These are additional incentives for slag sensor adoption.

Unfortunately, slag sensors tend to have a detection threshold of 10 to 20% slag in the outflow stream. Water model measurements by the present authors have shown that the percentage of oil in the outflow stream remains well under 1 to 5% through much of a vortexing funnel flow. Thus, it is unlikely that many slag sensors will be able to detect discrete slag entrainment events arising from weak residual rotational motions. Whether any such weak entrainment would indeed result in a higher inclusion count in the final product is open to debate.

A weakness of practically all vortexing funnel modelling studies to-date is that they have failed to either quantify the residual tangential velocity distribution, or maintain similarity with residual tangential motion likely to be prevalent in actual ladles, or both. Conclusions from such studies may, or may not be, conclusive. Thus, *a priori* knowledge of residual rotational motion in actual ladles is essential. A few mathematical models have been attempted to address this need, but there is much more that remains to be accomplished.[5,6,7] In light of these facts, conclusions such as those arrived at by Andrzejewski *et al.*[8] that slag entrainment from vortexing funnel formation can be discounted altogether is probably erroneous, in that the statement lacks universal applicability. Moreover, experiments carried out by the present authors in an approximately 1/2.4 scale model of a steelmaking ladle exposed to stirring and holding according to Froude similarity conditions, indicated the likelihood of weak residual rotational motions being present at the start of teeming. These then resulted in a vortexing funnel long before the non-vortexing funnel described by Andrzewjewski *et al.*[9]

Since it is impossible to monitor all of the product in high tonnage manufacturing, steel plants tend to have standard operating procedures that not only aim to ensure that all product will meet required cleanness specifications, but also to pro-actively detect and downgrade steel produced under non-standard operating conditions.

Thus, a clearer understanding of the mechanisms for vortexing and non-vortexing funnel formation can be very useful. This paper is a step in that direction. Dimensionless correlations for vortexing and non-vortexing funnel formation are discussed in detail. Hitherto unpublished results are presented to validate these correlations. Characteristic differences between the two modes of entrainment are discussed, and appropriate modelling criteria are outlined. More importantly, a *vortex buster* device is described that has been designed on the basis of the understanding gained from work carried out to-date.

2. Vortexing Funnel Formation

The classical explanation for the bathtub or kitchen-sink vortex is based on the principle of conservation of angular momentum.[10,11] A fluid particle on the surface of the vortex will conserve its angular momentum by progressively increasing its angular velocity as it spirals in towards the axis of rotation. At the very axis of this *free vortex,*[*] the particle will be spinning at an infinite velocity and will also have descended to a depth infinitely beneath the free surface.[12,13]

The free vortex solution is a steady-state solution, a state that is of least interest to the steelmaker intent on making clean steel without entraining any slag down the *vortexing funnel*. It is of greater interest to determine what does indeed happen between the start of teeming and the onset of vortexing, and why? What would be the critical height for the formation of a slag entraining vortexing funnel?

As it turns out, the critical height for vortexing funnel formation, $H_{cr,vf}$, is not a fundamental characteristic of the flow.[3] The time required, with reference to the start of teeming as time zero *(t= 0)*, for the residual tangential velocity in a small region surrounding the nozzle axis to increase from its initial value $V_{\theta,i}$ to a *critical value* $V_{\theta,cr}$, is a far more fundamental quantity. A *dimple* is first formed on the ladle liquid's surface at $t=t_{cr,dimple}$ and $H=H_{cr,dimple}$. The dimple then quickly extends its tail towards the drainage nozzle, and grows into a fully developed, air or slag-entraining, vortexing funnel as the liquid level in the ladle drops to $H_{cr,vf}$. The time $t_{cr,dimple}$[**] needed for the residual tangential velocity to accelerate to the so-called critical value was found not to depend on the diameter of the nozzle for any given ladle diameter.[3,14,15] Since the instantaneous liquid level remaining in the ladle does depend on the rate of outflow and the rate of change of liquid level, both $H_{cr,dimple}$ and $H_{cr,vf}$ are inversely proportional to the ratio of nozzle diameter to ladle diameter, d/D. In other words, starting from otherwise identical conditions (H_i, $V_{\theta,i}$, D, l, nozzle entrance geometry, *etc.*), the smaller the diameter of the nozzle the greater will be the value of $H_{cr,dimple}$ and $H_{cr,vf}$, and *vice versa*.[3,16,17,18]

Characteristic features of a vortexing funnel at its critical point are shown in Figure 1. A direct proportionality with the initial height H_i of liquid in the ladle was also observed.[3,19] The higher the value of H_i at the start of teeming, the higher were the critical heights for the formation of the dimple and the vortexing funnel, all other variables such as $V_{\theta,i}$, D and d remaining unchanged.

---

[*] Classical potential theory, or inviscid fluid flow theory, teaches us that a potential or free vortex can be obtained from the superposition of a line vortex and a line sink both sharing a common center. It can be shown that (a) streamlines of such a flow are logarithmic spirals, (b) the tangential velocity, $V_\theta \rightarrow \infty$ at r=0, and (c) the height of the vortex, h $\rightarrow \infty$ at $r=0$.[12]

[**] Parameters influencing $t_{cr,dimple}$ are yet to be studied in detail. However, it was observed in our experiments that $t_{cr,dimple}$ is strongly influenced by $V_{\theta,i}$ itself, as one would expect. We can also expect it to be influenced by the rate of change of liquid level (*i.e.*, d/D, l, H_i, nozzle geometry), and physical properties of the liquid particularly viscosity and density (one foresees a Reynolds number dependence here). Needless to say, a more fundamental understanding of the evolution of residual tangential velocity from an initial value (and distribution) to an as yet loosely-defined critical value (at small radii) can be of tremendous value in understanding non-steady state vortexing funnel formation.

A significant dependence on nozzle geometry was also observed. Nozzles with rounded entrance geometries offer less resistance to flow than sharp-edged nozzles, and the correspondingly higher instantaneous discharge flow rates from rounded entrance nozzles translated into proportionally lower values of $H_{cr,dimple}$ and $H_{cr,vf}$.

Several workers who studied vortexing funnel formation during non-steady state teeming limited themselves to describing the residual rotational motion on the basis of the holding time, t_{hold}.[8,17,20] A tangentially disposed filling inlet tube was used to autogenously induce rotational motion in the liquid during the ladle filling operation. Measurements showed that the radial distribution of angular velocity was markedly different at different holding times, and thus t_{hold} was a far simpler measure of residual rotation than $V_{\theta,i}$. For example, shortly after the end of filling, angular velocities were much larger at large radii than at smaller radii. However, the behaviour was quite the opposite at longer holding times. The tangential velocity distribution was thus neither that of rigid body rotation, nor that of a free vortex. Local values did show a steady decaying trend, and $H_{cr,vf}$ was found to decrease with increasing holding time. In experimental studies of steady-state vortexing funnels on the other hand, several authors were able to specify the intensity of residual motion in terms of a known (constant) circulation.[21,22,23,24,25]

An unique filling arrangement was developed by the current authors. While details are provided elsewhere,[3,14] a tangential velocity distribution was obtained that was more or less constant in the bulk of the ladle liquid; *i.e.*, $V_\theta(r,\theta,z) \neq f(r,\theta,z) =$ **a constant** at any given instant in time (except in the vicinity of the walls, where velocities were zero). The measured residual tangential velocity was found to decay asymptotically with increasing holding time, *i.e.*, $V_\theta(t) = C/t$, where C is a constant (see Figures 2 and 3). Thus it was possible to show that $H_{cr,dimple}$ and $H_{cr,vf}$ varied in direct proportion to a well-defined $V_{\theta,i}$. It was also possible to develop a dimensionless representation of the critical condition data.

2.1 Conditions favourable to vortexing funnel formation

A critical tangential velocity hypothesis was thus devised with the following necessary conditions:

(1) Some amount of residual tangential motion must be present in the ladle at the start of teeming.

(2) The axis of rotation of such pre-existing residual motions must be in reasonably good alignment with the axis of the (exit) teeming nozzle set in the base of the ladle.

(3) External means that could potentially destabilise vortexing funnel formation by countermanding condition (2) above should not be present (*i.e.*, vortex breakers, or electro-magnetically induced counter flows are absent).

During vortexing funnel flows, the bulk of the teeming outflow is drawn from an approximately cylindrical column above the nozzle (see also Figure 4). Maximum values for instantaneous downwards-axial velocities are prevalent along the axis of the nozzle (*i.e.*, at $r=0$). The principle of conservation of mass in the control volume requires that strong radial velocities are induced in the vicinity of the control volume. Tangential velocities at small radii are accelerated rapidly due to their interaction with these radial velocities (the Coriolis term in the unsteady state θ-momentum equation of the Navier-Stokes equation: $(V_\theta \cdot V_r)/r$). A dimple is initiated when the tangential velocity at small radius exceeds a critical value, and a fully developed vortexing funnel soon follows.

2.2 Dimensional analysis

Thus the following functional relationship can be written to describe the critical height for vortexing funnel formation in a teeming ladle fitted with a centrally located nozzle, and filled with a single phase liquid:

$$H_{cr,vf} = f(H_i, V_{\theta,i}, d, D, \rho, \mu, g) \qquad \textbf{(1)}$$

where ρ is the density of the liquid being teemed, μ is its viscosity, and g is the acceleration due to gravity, respectively. Invoking the Buckingham π theorem, and using H_i, ρ, and g as the common variables, the following five π groups can be obtained from Eq. (1).

$$\pi_1 = \frac{H_{cr,vf}}{H_i} \qquad \pi_2 = \frac{d}{H_i} \qquad \pi_3 = \frac{D}{H_i}$$

$$\pi_4 = \frac{V_{\theta,i}}{\sqrt{g\,H_i}} \approx \frac{V_{\theta,i}}{V_{out,i}} \quad \text{(Vortex Number; a Froude number)}$$

$$\pi_5 = \frac{\rho\,H_i\sqrt{g\,H_i}}{\mu} \approx \frac{\rho\,V_{out,i}\,H_i}{\mu} \quad \text{(Reynolds number)}$$

where $V_{out,i}$ is the outflow velocity at the start of teeming. π_1 is the primary dependent variable. π_2 and π_3 represent geometric similarity ratios, which could be combined into one, *viz.*, $\pi_2/\pi_3 = d/D$. π_4 is the *vortex number* representing the ratio of initial tangential velocity to the initial outflow velocity at the start of teeming. As seen, the *vortex number* has the form of a Froude number. The Reynolds number effect of π_5 was neglected in the present study.

2.3 Results and Discussion of Scale-up Experiments

Vortexing funnel formation experiments were carried out in geometrically similar Plexiglas® ladles, of diameter 495 mm and 1160 mm respectively (geometric scale factor, λ = 0.427). Plexiglas® nozzles were used that were geometrically similar in all respects, including their entrance geometry. Further details of the experimental conditions are provided in Table 1.

Tangential velocity decay behaviour measured in the 495 mm and 1160 mm diameter ladles are shown in Figures 2 and 3, respectively. Raw experimental data are plotted in Figures 5 and 6. Figure 5 shows the variation of $H_{cr,dimple}$ and $H_{cr,vf}$ against $V_{\theta,i}$ in the 495 mm diameter ladle. Figure 6 is the equivalent plot for the 1160 mm diameter ladle. As seen, the difference between $H_{cr,dimple}$ and $H_{cr,vf}$ is minimal at large values of $V_{\theta,i}$ (the vortexing funnel is formed more or less instantaneously, mere seconds separating its formation from that of the dimple). At lower values of $V_{\theta,i}$, the progression from the initial dimple to the fully developed vortexing funnel is much slower; the difference between the two critical heights ranged from 80 to 120 mm at low values of $V_{\theta,i}$, in the range of 5 to 20 mm/s; intermittent entrainment of discrete air bubbles was observed as the dimple length alternately grew and shrank before finally becoming a fully developed vortexing funnel.

Dimensionless critical heights for dimple and vortexing funnel formation are plotted against $V_{\theta,i}$ in Figures 7 and 8, respectively. The behaviour in the two geometrically similar ladles is very close to one another, and in general, $H_{cr,dimple}$ and $H_{cr,vf}$ quickly reach 70 to 80% of the initial height at $V_{\theta,i}$ values less than 20 to 30 mm/s.

Dimensionless critical heights are plotted against the Vortex Number in Figures 9 and 10. A sharply rising curve is seen at small values of the Vortex number, quickly reaching 80% or 90% of the initial height before a Vortex Number value of unity is reached.

Clearly the data confirm the validity of the dimensional analysis. The critical condition behaviour is best described by three separate equations for three ranges of vortex number:

$0 < \textit{vortex number} \leq 0.05$ (non-vortexing funnel regime)

$0.05 <$ vortex number < 1

vortex number > 1

2.3.1 Significance of the Vortex Number

The Vortex Number can be interpreted as a measure of the angular momentum of the liquid exiting the ladle. The lower the angular momentum in the outflow, the lower will be the propensity to form a vortexing funnel. Even trace amounts of angular momentum in the outflow stream are likely to significantly increase the propensity to form a vortexing funnel. The presence of strong angular momentum in the outflow stream manifests itself as a visibly bulged outflow stream. Compact outflow streams are thus desirable as they are indicative of negligible angular momentum in the outflow.

It is reasonable to expect that liquid viscosity will increase a fluid's resistance to accelerating rotational flows at small radii, and limit these to a critical value. Similarly, tangential velocity is likely to decay more rapidly with increasing holding time in viscous liquids. Further experiments to elucidate the role of Reynolds number are needed to further refine the correlations now presented. However, from the point of view of minimizing slag entrainment it may be useful to explore means of suppressing vortexing funnel formation altogether, irrespective of the residual rotation present in the ladle.

2.3.2 A novel method for suppressing vortexing funnel formation

The introduction of a horizontal baffle plate directly above the nozzle will help sever fluid communications between the rotating liquid in the ladle and the outflow. The diameter of the baffle plate, and the gap between the underside of the baffle plate and the ladle bottom were both optimized. In addition, it was necessary to streamline the radial flow towards the nozzle axis in order to ensure that it was free of all traces of rotational motion. With these modifications, the shape of the control volume feeding the outflow resembled a flat disc rather than a cylinder spanning the entire column of liquid.

Such a flow modification device, or *vortex buster*, has been proven through trials in laboratory water models as well as in an actual steelmaking tundish.[19] Figure 11 shows a photograph of a *vortex buster* built for water model trials, and its effectiveness in suppressing vortexing funnel formation for a wide range of $V_{\theta,i}$ values is shown in Figure 12.[3] A refractory *vortex* buster is shown in Figure 13, being pre-heated in preparation for a casting trial; as reported elsewhere, significant improvements in steel cleanness were obtained during these trials.[19]

2.3.3 Vortexing Funnel Formation during teeming through off-centred nozzles

Steelmaking ladles are typically teemed through nozzles positioned eccentrically, 2/3 radius being the most common location for the nozzle. Given the absence of the necessary condition (2), *i.e.*, alignment between the axis of rotation (centred about the ladle axis) and the axis of the teeming nozzle, the observation of Sucker *et al.*18 that the critical height for vortexing funnel entrainment decreases with increasing eccentricity of the teeming nozzle is not surprising. A similar result was obtained in the present work as well in trials with 374 mm diameter ladles, with $V_{\theta,i}$ values greater than 40 mm/s.[14] For lower values of $V_{\theta,i}$, in the range 10 to 30 mm/s, $H_{cr,vf}$ values were 5 to 8 times larger than $H_{cr,vf}$ values obtained at $V_{\theta,i} > 40$ mm/s, and yet were

considerably lower than the equivalent values for central nozzle drainage (see Figure 14). This tendency to form taller vortexing funnels at weaker $V_{\theta,i}$ values was even more pronounced in trials in a larger, 1160 mm diameter ladle, where the axis of rotation was found to progressively gravitate towards the axis of the off-centred nozzle throughout the teeming. $H_{cr,vf}$ values for $V_{\theta,i}$ in the range 10 to 30 mm/s approached values obtained for central nozzle drainage, as seen in Figure 15.

A few trials were carried out in a 1/2.4-scale model of an 80-ton steelmaking ladle, wherein argon stirring influenced residual rotational motion. Its decay during the holding period, and its evolution during subsequent teeming, was studied under Froude similarity conditions. A tendency towards vortexing funnel entrainment was observed in these trials when 100 to 150 mm of water remained in the ladle (240 to 360 mm of steel). Additional trials in full-scale models may be necessary to obtain further confirmation of these preliminary results.

At the same time, it was found that a properly designed *vortex buster* was also capable of suppressing vortexing funnel formation in larger ladles with eccentric nozzles.

2.3.4 Influence of an oil (slag) layer on vortexing funnel formation

In the case of non-vortexing funnel formation, presented in greater detail in Section 3, conclusive evidence was obtained, theoretically as well as with experiment measurements, that the critical height for non-vortexing funnel formation, $H_{cr,nvf}$ varied in inverse proportion with $(1 - \rho_2/\rho_1)$. In other words, $H_{cr,nvf}$ would have a higher value with oil as the lighter phase liquid compared to air as the supernatant fluid. This can be explained on the basis of the buoyancy forces needed to prevent an entrainment of oil being lower than those to entrain air. A similar behaviour can also be expected to be valid for vortexing funnel entrainment.

A limited number of oil-entraining vortexing funnel experiments were carried out in a 374 mm diameter ladle. $H_{cr,dimple}$ and $H_{cr,vf}$ values were definitely higher with the oil layer (as the supernatant fluid) than with air, for all $V_{\theta,i}$ values in excess of 30 mm/s (see Figures 16 and 17, respectively). The lateral dimensions of the oil-entraining vortexing funnel were found to be significantly larger than the air-entraining vortexing funnel formed under otherwise identical geometric and initial conditions. For lower values of initial tangential velocity, *i.e.*, $V_{\theta,i} < 30$ mm/s, the critical height at which the oil-entraining vortexing funnel became fully developed turned out to be slightly lower than the equivalent air-entraining vortexing funnel, even though the $H_{cr,dimple}$ values had been similar for air and oil. However, a series of large oil droplets were carried away from the lingering tail of the dimple into the outflow, in an intermittent fashion; this entrainment constituted only 1% to 5% of the total volumetric outflow until after the oil-entraining vortexing funnel had become fully developed. Figure 18 shows an example of this intermittent entrainment.[3]

Additional trials may be needed, in larger diameter ladles, to confirm and validate these findings, and also include these into the dimensionless correlations. It has already been confirmed that a properly designed *vortex buster* device was capable of suppressing any and all oil-entrainment.

2.3.5 Scale-up and other considerations

A key finding of the above-mentioned studies that should be of interest to steelmakers is that a partial closure of the slide-gate opening after detection of slag entrainment will be counter-productive in the event that the entrainment had been a result of vortexing funnel formation. On the other hand, if measurements were to suggest that choking of the outflow rate does result in a reduction in the slag flow, the slag entrainment mechanism is unlikely to be that of a vortexing funnel. It will be shown in the following sections that under favourable conditions, reducing the outflow rate could lower the critical height for non-vortexing funnel formation.

A better understanding of the residual rotational motion prevalent in teeming ladles is required. Full-scale model trials, supplemented with appropriate mathematical modelling, will be useful.

3. Non-Vortexing Funnel Formation

In the absence of residual rotational motion in the teeming ladle, much of the liquid leaving the ladle is drawn from the vicinity of a hemispherical region (control volume) surrounding the nozzle entrance (contrary to the narrow cylindrical control volume in the case of a vortexing funnel). When the sum total of the flow entering normal to the control volume becomes less than the outflow capacity of the nozzle, then the supernatant fluid (liquid or gas) has to be entrained to form a non-vortexing funnel.

Characteristic features of a non-vortexing funnel at the critical point are shown in Figure 19.[3] $H_{cr,nvf}$ is known to vary linearly with the diameter d of the nozzle, ranging in value from $0.5d$ to $3d$. $H_{cr,nvf}$ is also known to vary in direct proportion with the outflow rate; *i.e.*, the longer the nozzle, the higher was $H_{cr,nvf}$; sharp-edged nozzles showed a higher $H_{cr,nvf}$ than nozzles with a rounded entrance geometry, other parameters remaining unchanged. On the other hand, $H_{cr,nvf}$ is known to be independent of ladle diameter D, eccentricity of the nozzle (centrally located on the ladle bottom, or not), the shape of the vessel's bottom (flat- or hemispherical-bottomed,[26] sloped or inclined[8,20,27]), and the initial height of liquid, H_i, in the ladle at the start of teeming.[3]

3.1 Dimensional Analysis

The following functional relationship can be written to describe the critical height for non-vortexing funnel formation in a teeming ladle fitted with a nozzle on its floor:

$$H_{cr,nvf} = f(d,\ Q_{out}\ ,\ \rho_1\ ,\ \rho_2\ ,\ g\ ) \qquad \textbf{(2)}$$

where Q_{out} is the outflow rate, ρ_1 and ρ_2 are the densities of the liquid being teemed and the supernatant fluid (slag or air), and g is the acceleration due to gravity, respectively. Invoking the Buckingham π theorem, and using d, ρ_1, and g as the common variables, the following three π groups can be obtained from Eq. (2):

$$\pi_1 = \frac{H_{cr,nvf}}{d} \qquad \pi_2 = \frac{\rho_2}{\rho_1}$$

$$\pi_3 = \frac{Q_{out}^2}{g\,d^5} \qquad \text{(Froude number)}$$

where π_1 is the dependent variable, π_2 represents the relative density of the supernatant fluid (liquid or gas), and π_3 is the primary independent variable. In other words:

$$\frac{H_{cr,nvf}}{d} = f\left(\frac{Q^2_{cr,nvf}}{g\,d^5},\ \frac{\rho_2}{\rho_1}\right) \quad \textbf{(3)}$$

3.2 Critical Condition Models

The critical condition for non-vortexing funnel formation has been analyzed mathematically using various assumptions including inviscid and incompressible fluids, irrotational flow, hemispherical control volume around the nozzle with iso-normal velocities (see Figure 20), *etc.* Both Lubin and Springer[28] and Harleman *et al.*[29] arrived at more or less equivalent critical condition models. Thus, the critical height for non-vortexing funnel formation could be described by:

$$\frac{H_{cr,nvf}}{d} = \left[\frac{1}{2.54\,K}\cdot\frac{Q_{cr,nvf}}{\sqrt{g\left(1-\frac{\rho_2}{\rho_1}\right)d^5}}\right]^{0.4} \quad \textbf{(4)}$$

where K is the empirical, Harleman constant. While Lubin and Springer[28] obtained complete agreement between experimental measurements and mathematical model (*i.e.*, K was 1 and so dropped out of the equation), Harleman *et al.*[29] could only obtain a good fit between measurements and theory by assuming a value of 0.64 for K. Harleman *et al.* concluded that K was related to flow losses in the drainage system, and that K could not exceed a value of *unity*. However, as seen in Figure 21, it has since been verified that K can indeed have a value greater than *unity*.[3,16] With such an interpretation for K, albeit empirical, experimental observations made by a number of authors that had appeared to deviate significantly from Eq. (4) could now be explained.

3.3 Influence of Viscosity

A key assumption of the critical condition model Eq. (4) is that the liquid being teemed as well as the supernatant fluid (liquid or gas) both behave as inviscid fluids. Lubin and Springer[28] confirmed the validity of their model using lighter phase liquids with viscosities ranging from 1.3 to 60 cP, maintaining water as the primary liquid. Gluck *et* al.[26] also found a lack of dependence on viscosity in trials where they varied the viscosity of the teeming liquid, maintaining air as the lighter phase.

The question is often raised whether, or not, a crusty slag would resist entrainment better than a more fluid, liquid slag. Lime additions, typically made to steelmaking slags to increase their fluidity, also tend to increase slag density (the density of lime additions range from 3250 to 3380 kg/m^3 , versus 2200 to 2400 kg/m^3 for silica).

In order to lay this question to rest, a set of experiments were carried out wherein the relative viscosity of the supernatant fluid w.r.t. that of the primary liquid, *i.e.*, μ_2/μ_1 , was varied widely from 35 to 10,000.[30] Viscosity and density data for a few selected carbon steels and slags are given in Table 2. The relative density of typical steelmaking slags, vis-à-vis that of (liquid) carbon steels, ranges from 0.28 to 0.43, while their relative viscosities vary between 80 and 600. The primary liquid-supernatant liquid combinations studied in laboratory trials are listed in Table 3, and key experimental conditions are listed in Table 4. The results of these trials clearly proved the lack of dependence of $H_{cr,nvf}$ on μ_2/μ_1 (see Figure 22).

3.4 Relative density of light phase fluid (liquid or gas)

Eq. (4) clearly shows the dependence of $H_{cr,nvf}$ on the density difference between the supernatant fluid (liquid or gas) and the liquid being teemed. The closer the density of the supernatant liquid to that of the primary liquid, the higher will be the value of $H_{cr,nvf}$. Assuming $Q_{cr,nvf}$ and d will remain unchanged, the impact of increasing the relative density of the supernatant phase can be obtained by rearranging Eq. (4):

$$\% \text{ change in } \frac{H_{cr,nvf}}{d} = 100\left(\left(\frac{\rho_1}{\rho_1 - \rho_2}\right)^{0.2} - 1\right) \qquad \textbf{(5)}$$

Eq. (5) is plotted in 23. $H_{cr,nvf}/d$ for $\rho_2/\rho_1 = 0.999$ will be nearly four times the value of $H_{cr,nvf}/d$ for $\rho_2/\rho_1 \cong 0$. Assuming the density of liquid steel and liquid slag to be 7000 and 3000 kg/m^3, respectively, Eq. (5) states that $H_{cr,nvf}/d$ for a "steel-slag" system will be approximately 11.8% higher than the $H_{cr,nvf}/d$ for an equivalent "water-air" system.

Andrzejewski *et al.*[8] found that the $H_{cr,nvf}$ predicted on the basis of (a) a critical model that did not include the relative density term, and (b) full-scale water model trials, was about 13.2% lower than the value measured in the steelmaking ladle, quite in line with the projections of Eqs. (4) and (5). While Andrzejewski *et al.*[8] dismissed this difference as minor, and within the limits of experimental error, the discrepancy was most likely explainable on the basis of the relative density term having been excluded from their mathematical model. Had it been included, there should have been a better fit between predicted and measured values.

3.5 Similarity criteria and scale-up considerations

Unless teeming can be ended in a timely manner, slag entrainment through a non-vortexing funnel will occur, whether it is preceded by a vortexing funnel or not, irrespective of the presence or absence of adventitious rotational motion in the teeming ladle. As the theoretical lower limit to which the liquid steel in the ladle could possibly be lowered during teeming without entraining slag, knowledge of $H_{cr,nvf}$ is critical.

Full-scale water model simulation of ladle teeming can provide useful information about the impact of slide gate position on $H_{cr,nvf}$. Such knowledge will be particularly useful since nozzle characteristics are not explicitly included in Eq. (4). Since Reynolds number similarity will be automatically satisfied, full-scale model trials will also ensure that any secondary dependence of $H_{cr,nvf}$ on Reynolds number will be properly accounted for. Knowledge of the critical height for the onset of air-entraining non-vortexing funnel flow for a range of teeming conditions can then be scaled-up into a $H_{cr,nvf}$ value for entrainment of slag, using Eq. (5).

Figure 24 shows the influence of slide gate opening on $H_{cr,nvf}$ during teeming. In these trials, a 1:1 (full-scale) model of the teeming nozzle, gate and shroud arrangement used in an 80-ton steelmaking ladle was fitted into a 495 mm diameter ladle. These water model trials showed that (a) $H_{cr,nvf}$ will be higher for submerged pouring than for open pouring and (b) a *vortex buster* (VB) device, designed according to the principles outlined in Section 2.3.2, is also extremely beneficial in delaying the onset of a non-vortexing funnel. As seen, the VB can bring about a two to three-fold reduction in $H_{cr,nvf}$ compared to the case of a standard nozzle and shroud arrangement.

By its very design, the VB promotes rotation-free radial flow towards the nozzle axis. By so reinforcing the inclination of the liquid to flow along the direction of maximum pressure

gradient (close to, and parallel to, the vessel bottom), the VB design successfully delays the onset of the critical condition where the incoming liquid is no longer able to fully satisfy the drainage potential of the teeming nozzle. The benefits of such a flow modifier include cleaner steel in tundishes.[19]

4. Summary and Conclusions

Experimental observations in water model studies of vortexing funnel formation are explained in terms of a critical tangential velocity hypothesis.

Dimensionless relationships between key variables affecting the critical height for vortexing and non-vortexing funnel formation are described and validated.

Key characteristics of the two types of entrainment are described that should be useful to operators in identifying the slag entrainment mechanism that is likely prevalent, and develop counter-measures accordingly.

It has been shown that even weak, adventitious, residual rotational motion in the ladle could result in the formation of a slag entraining vortexing funnel. A *vortex number* value much less than unity is shown as sufficient to cause substantial vortexing. Vortexing funnel induced slag entrainment may be difficult to detect with existing slag sensing technologies, since the % slag (oil) in the outflow stream was measured as significantly lower than known minimum detection thresholds.

It has been pointed out that sufficient information may be unavailable yet to make a quantitative assessment of the respective contributions of vortexing funnels and non-vortexing funnels, or even that vortexing funnel is a definite contributor to slag entrainment in teeming ladles. Conditions favourable to non-vortexing funnel formation definitely become prevalent in every ladle that is teemed.

It is shown that a *vortex buster* device designed on the basic understanding gained from vortexing funnel formation studies is also capable of reducing slag entrainment arising from non-vortexing funnel formation. Thus, a *vortex buster* device is capable of playing a dual role. First and foremost, it can help maximise yield and minimise slag entrainment during late-stage teeming (non-vortexing funnel regime). Additionally, it can provide excellent insurance against adventitious vortexing funnels and any associated loss of steel cleanness.

References

1. M. Byrne, A.W. Cramb and T.W. Fenicle, "The sources of exogenous inclusions in continuous cast, aluminum-killed steels," Proceedings of the 68th Steelmaking Conference, ISS-AIME, 1985, pp. 451-461
2. A.W. Cramb and M. Byrne, "Tundish slag entrainment at Bethlehem's Burns Harbor (Indiana) slab caster," Proceedings of the 67th Steelmaking Conference, ISS-AIME, 1984, pp. 5-13
3. Ramani Sankaranarayanan, "Modeling of Slag Entraining Funnel Formation ('vortex') during liquid metal transfer operations," Ph.D. Thesis, McGill University, Montreal, Québec, Canada, October 1994
4. H. Jacobi and K. Wünnenberg, 7th Japan-Germany Seminar, Düsseldorf, May 1987
5. G.G. Roy, V. Sing and D. Mazumdar, "On the mathematical modelling of turbulent fluid flow in filling ladles," Transactions of the Indian Institute of Metals, Vol. 45, No. 3, June 1992, pp. 147-152

6. D. Mazumdar and R.I.L. Guthrie, "Discussion of 'Decay of Fluid Motion in a Filling Ladle after Tapping,'" Metallurgical and Materials Transactions B, Vol. 30B, No. 3, June 1999, pp. 541-543B
7. G.G. Roy, "Decay of fluid motion in a filling ladle after tapping," Metallurgical and Materials Transactions B, Vol. 29B, No. 4, Aug. 1998, pp. 931-935B
8. P. Andrzejewski, A. Diener and W. Pluschkell, "Model investigations of slag flow during last stages of ladle teeming," Steel Research, Vol. 58, No. 12, 1987, pp. 547-552
9. R. Sankaranarayanan and R.I.L. Guthrie, MMPC Internal Report No. 44, McGill University, 1996
10. Henry A.Rowland , "The Vortex Problem," The Scientific American, 13:308, October 1865, pp. 308
11 E.N. Da C. Andrade, "Whirlpools and Vortices," Proceedings of the Royal Institute of London, Vol. 29, 1936, pp. 320 (see also, The Royal Institute Library of Science, Vol. 10, Elsevier Publishing Company Limited, 1970, pp. 178-200)
12. F.M. White, "Fluid Mechanics," McGraw Hill, Second Edition, 1979
13. R.I.L. Guthrie, "Engineering in Process Metallurgy," Clarendon Press, Oxford, 1989
14. R. Sankaranarayanan and R.I.L. Guthrie, "Slag entrainment through a 'funnel' vortex during ladle teeming operations," Proceedings of the International Symposium on Developments in Ladle Steelmaking and Continuous Casting, CIM-MetSoc, August 1990, pp. 66-87
15. R. Sankaranarayanan and R.I.L. Guthrie, "A laboratory study of slag entrainment during the emptying of metallurgical vessels," Proceedings of the 1992 Steelmaking Conference, ISS-AIME, Vol. 75, 1992, pp. 655-664
16. R. Sankaranarayanan and R.I.L. Guthrie, "Slag entrainment through a 'funnel' vortex during ladle teeming operations," Proceedings of the International Symposium on Developments in Ladle Steelmaking and Continuous Casting, CIM-MetSoc, August 1990, pp. 66-87
17. P. Hammerschmid, K.-H. Tacke, H. Popper, L. Weber, M. Dubke and K. Schwerdtfeger, "Vortex formation during drainage of metallurgical vessels," Ironmaking and Steelmaking, Vol. 11, No. 6, 1984, pp. 332-339
18. D. Sucker, J. Reinecke and H. Hage-Jewasinski, Stahl und Eisen, Vol. 105, No. 14/15, 1985, pp. 765-769
19. R. Sankaranarayanan and R.I.L. Guthrie, "Vortex suppression device improves steel cleanness," Proceedings of the Electric Furnace Conference, New Orleans, ISS-AIME, 1995, pp. 87-100
20. R. Steffen, "Fluid flow phenomena of metal and slag during drainage of metallurgical vessels," Proceedings of the International Conference on Secondary Metallurgy, Aachen, West Germany, September 1987, Preprints, pp. 97-118
21. J.C. Stevens and R.C. Kolf, "Vortex flow through horizontal orifices," Transactions of the ASCE, Vol. 124, 1959, Paper 3004, pp. 871-893
22. K. Haindl, "Contribution to air entrainment by a vortex," International Association of Hydraulic Research, 8th Congress, Montreal, 1959, Paper 16-D, pp. 1-17
23. M.C. Quick, "Scale relationships between geometrically similar Free Spiral Vortices (Part I)," Civil Engineering and Public Works Review, Vol. 57, Sept. 1962, 674, pp. 1135-1138
24. M.C. Quick, "Scale relationships between geometrically similar Free Spiral Vortices (Part II)," Civil Engineering and Public Works Review, Vol. 57, Oct. 1962, 675, pp. 1319-1320
25. L.L. Daggett and G.H. Keulegan, "Similitude in free-surface vortex formation," Proceedings of the ASCE, Journal of the Hydraulics Division, Vol. 100, HY11, November 1974, pp. 1565-1568
26. D.F. Gluck, J.P. Gille, D.J. Simkin and E.E. Zukoski, "Distortion of the liquid surface during tank discharge," Journal of Spacecraft and Rockets, Vol. 3, No. 11, 1966, pp. 1691-1692
27. R.I.L. Guthrie, H.B. Kim and R.Sankaranarayanan, McGill Metals Processing Centre (MMPC) Internal Report No. 54, McGill University, 1997
28. B.T. Lubin and G.S. Springer, "The formation of a dip on the surface of a liquid draining from a tank," Journal of Fluid Mechanics, Vol. 29, Part 2, 1967, pp. 385-390

29. D.R.F. Harleman, R.L. Morgan and R.A. Purple, "Selective withdrawal from a vertically stratified fluid," International Association for Hydraulics Research, 8th Congress, Montreal, 1959, Paper 10-C, pp. 1-16
30. D. Fargier, A.-J. Labouthie, R. Sankaranarayanan and R.I.L. Guthrie, McGill Metals Processing Centre (MMPC) Internal Report No. 34, McGill University, 1995

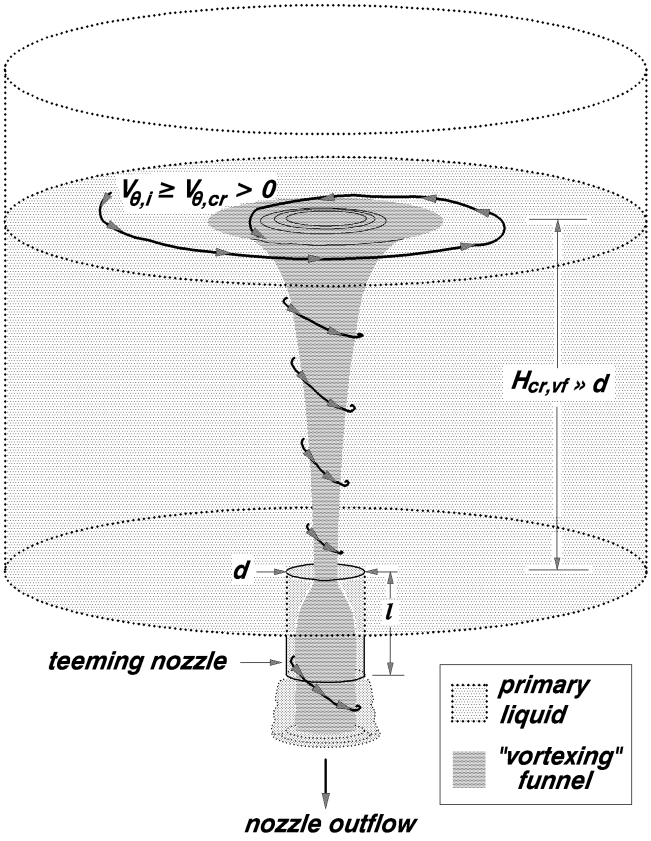

Figure 1: Characteristic features of a vortexing funnel at the critical point of its formation

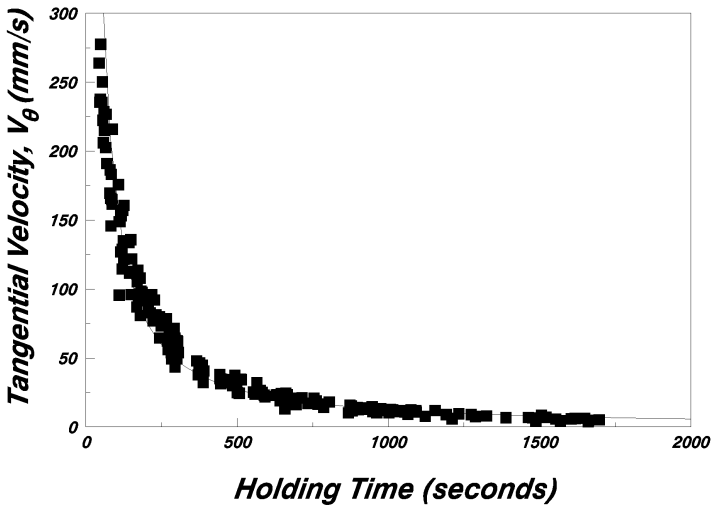

Figure 2: Measured decay in the tangential velocity vs. holding time (*D=495 mm*, H_i*=425 mm*)

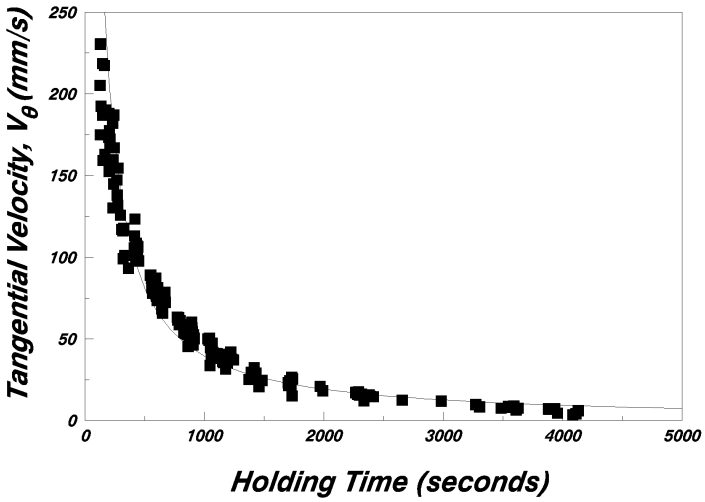

Figure 3: Measured decay in the tangential velocity vs. holding time (*D=1160mm, H_i=995mm)*

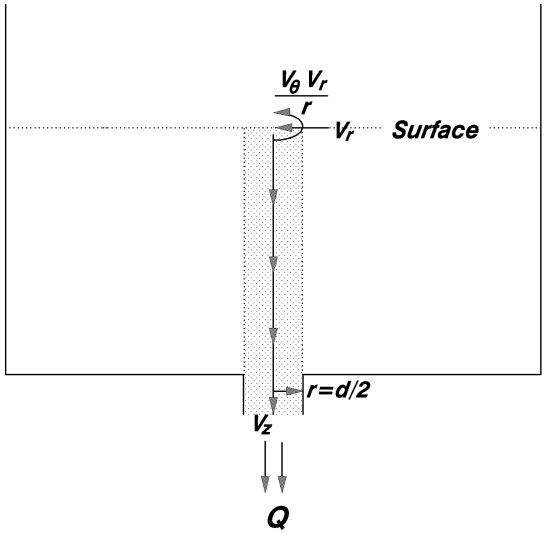

Figure 4: Schematic representation of interactions between downwards-axial, radial and tangential velocities in a narrow cylindrical control volume surrounding the nozzle during vortexing funnel flow.

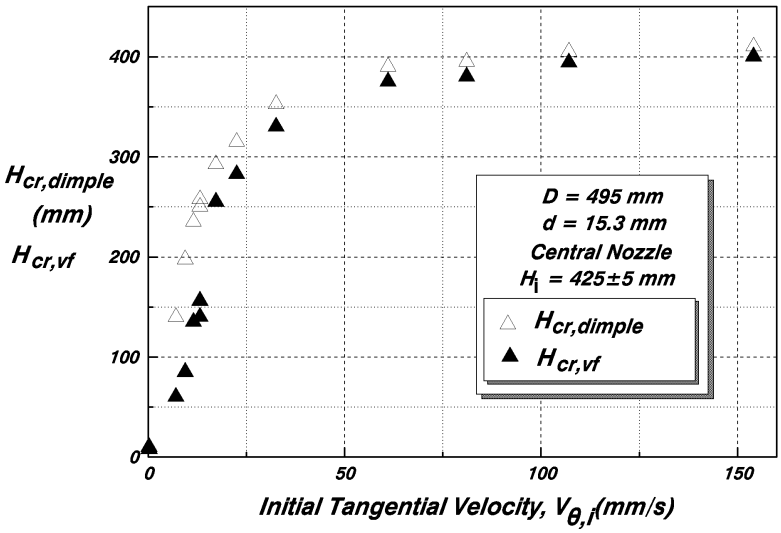

Figure 5: Critical heights for dimple and vortexing funnel formation in 495 mm diameter ladle

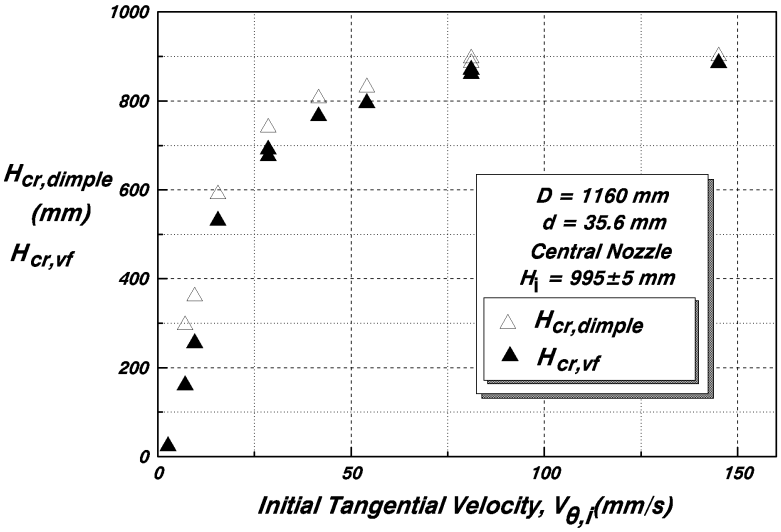

Figure 6: Critical heights for dimple and vortexing funnel formation in 1160 mm diameter ladle

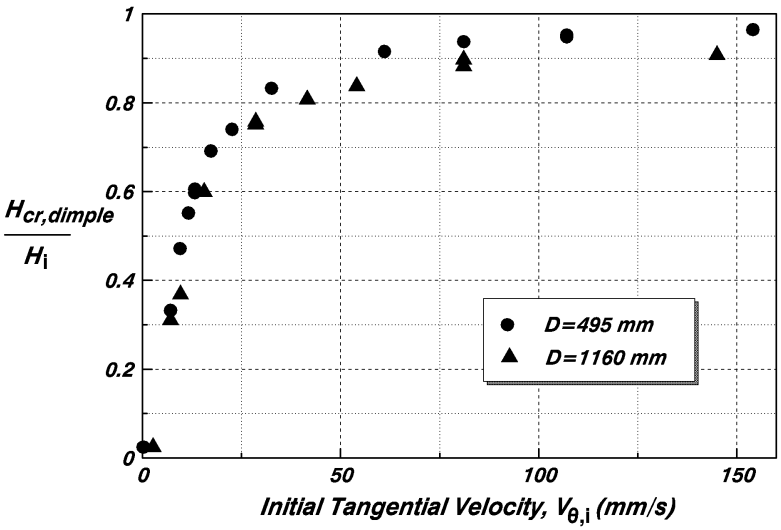

Figure 7: Dimensionless critical height for dimple formation vs. $V_{\theta i}$

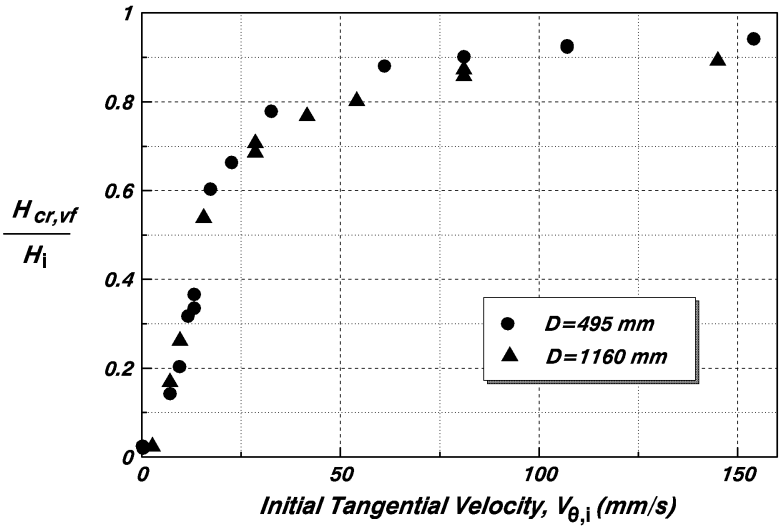

Figure 8: Dimensionless critical height for vortexing funnel formation vs. $V_{\theta i}$

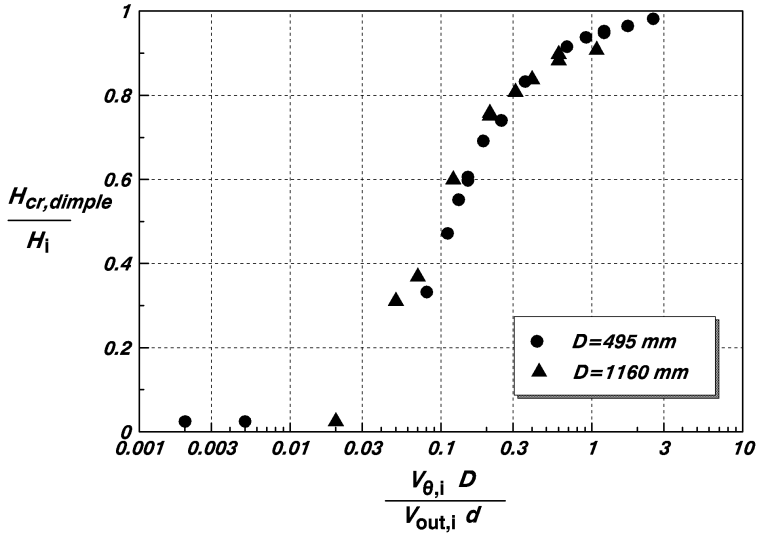

Figure 9: Critical height for dimple formation vs. the *vortex number*

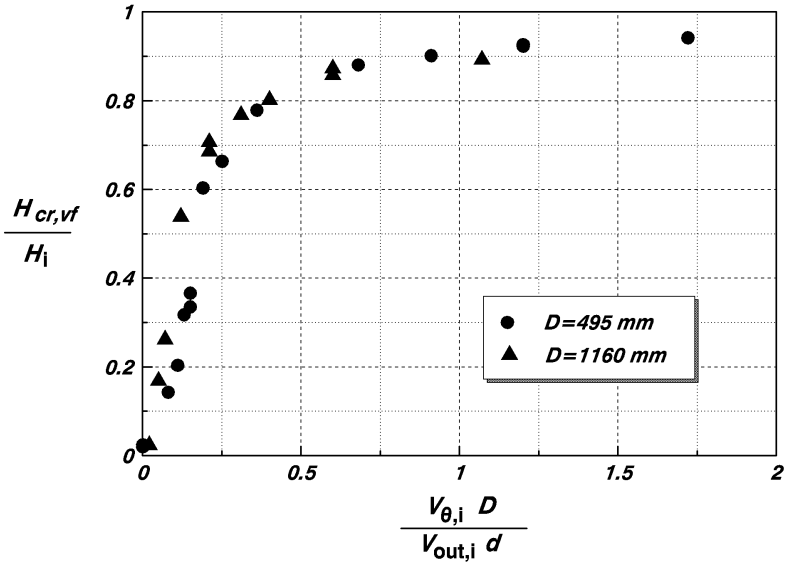

Figure 10: Critical height for vortexing funnel formation vs. *vortex number*

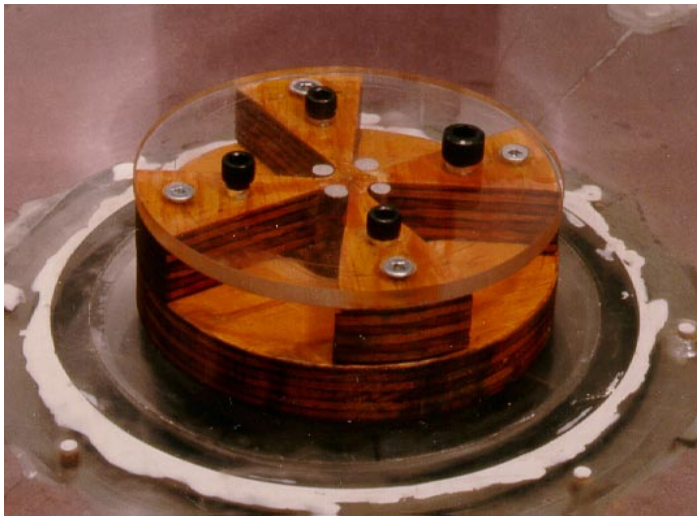

Figure 11: *Vortex Buster* designs were optimised in water model trials.[3]

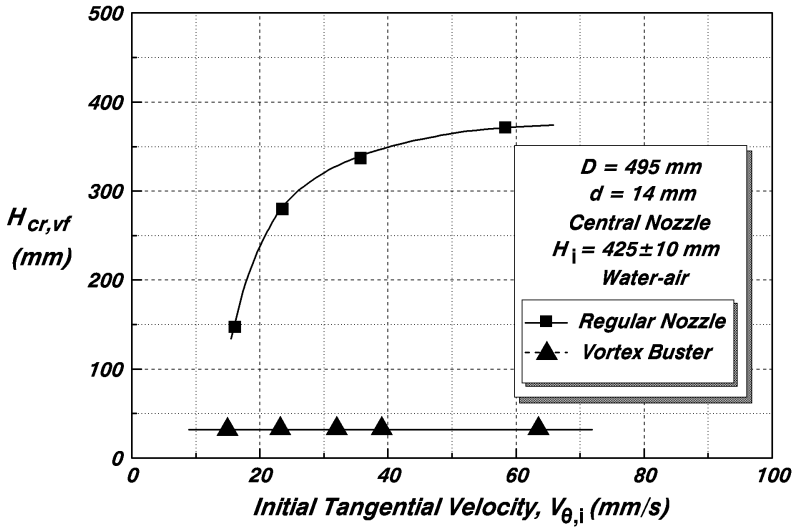

Figure 12: *Vortex Buster* shown in Figure 11 effectively suppressed vortexing funnel formation

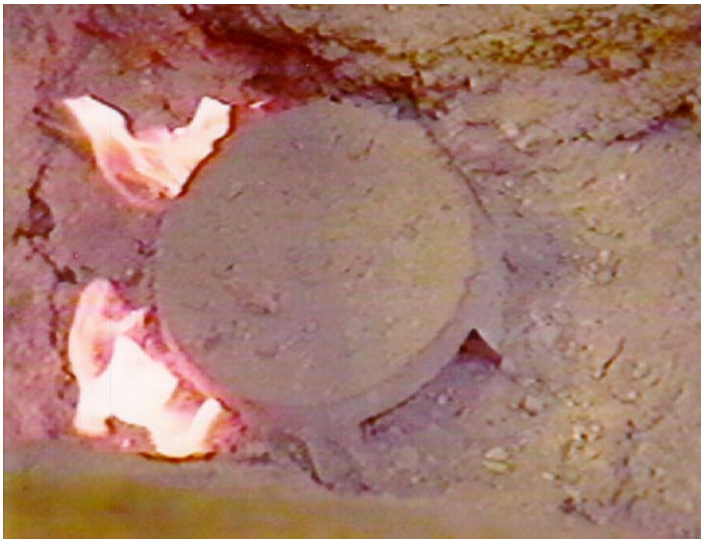

Figure 13: A refractory *Vortex Buster* being pre-heated prior to a casting trial in 12 ton tundish

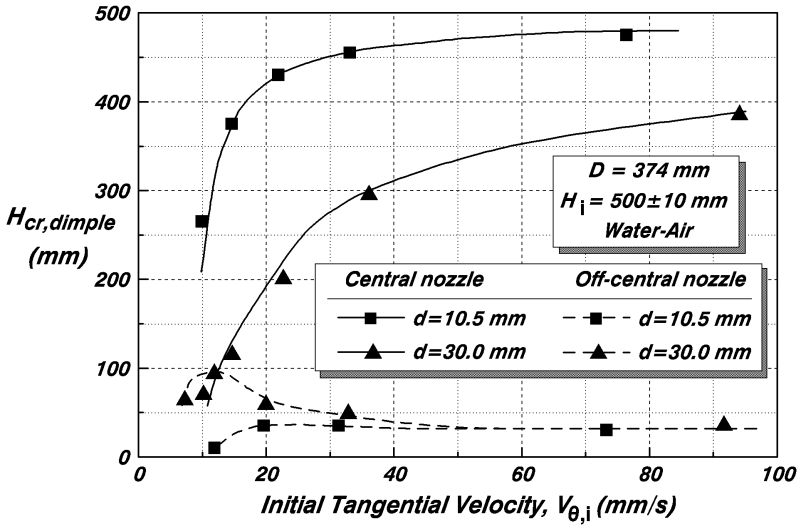

Figure 14: Teeming through central and eccentric nozzles: $H_{cr,dimple}$ vs. $V_{\theta,i}$ (D=374 mm)

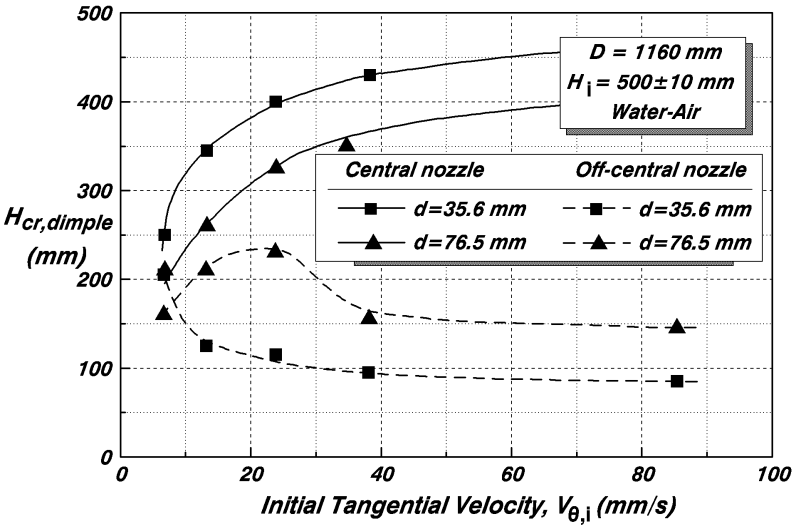

Figure 15: Teeming through central and eccentric nozzles: $H_{cr,dimple}$ vs. $V_{\theta,i}$ (D=1160 mm)

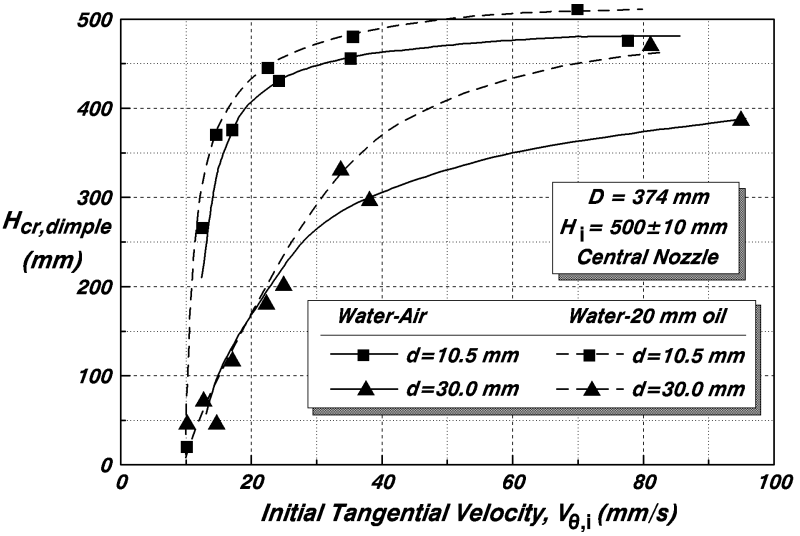

Figure 16: Oil (slag) versus air as supernatant fluid: $H_{cr,dimple}$ vs. $V_{\theta,i}$ (D=374 mm)

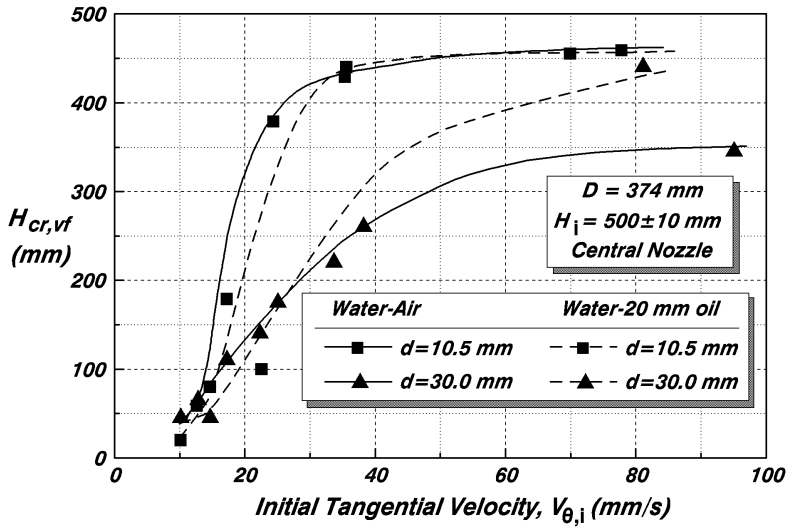

Figure 17: Oil (slag) versus air as supernatant fluid: $H_{cr,vf}$ vs. $V_{\theta i}$ (D=374 mm)

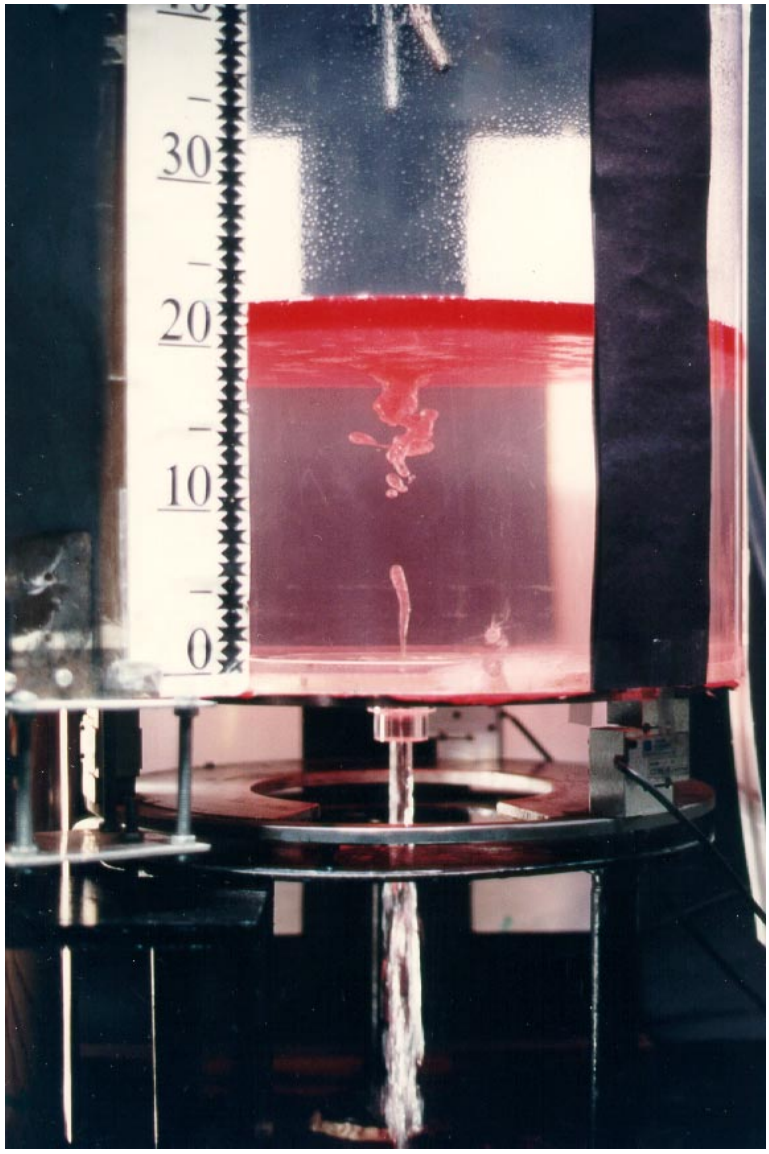

Figure 18: Discrete slag entrainment was often observed during teeming with weak $V_{\theta i}$

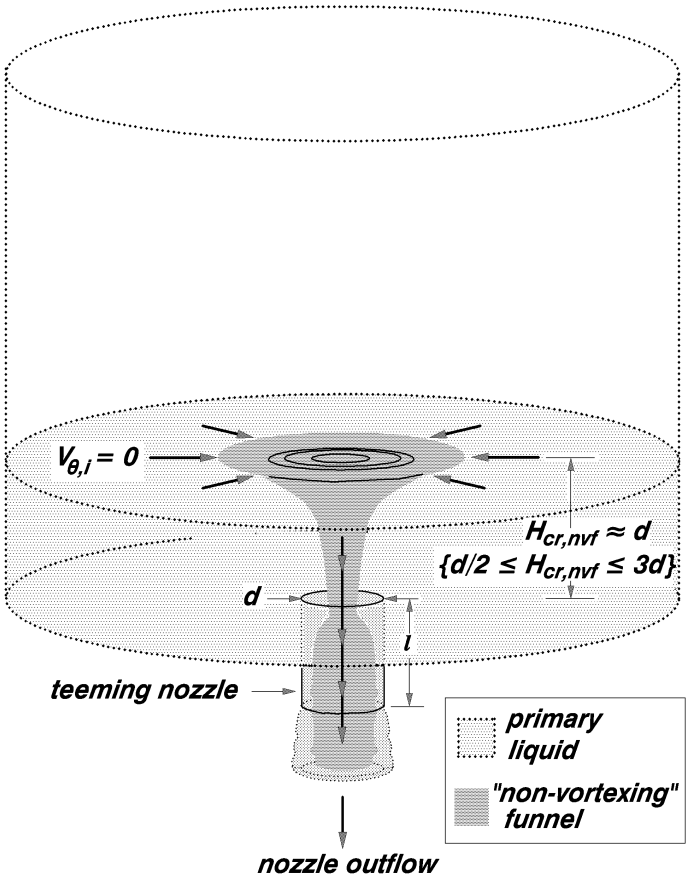

Figure 19: Characteristic features of a non-vortexing funnel at the critical point of its formation

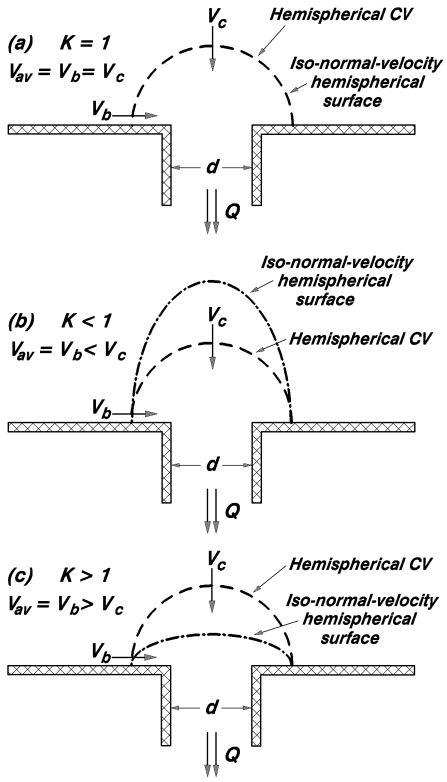

Figure 20: A schematic of flow velocities in the non-vortexing funnel control volume (a) Lubin and Springer model *(K=1)* (b) Harleman *et al.* model *(K<1)* and (c) extended model *(K>1*[3]

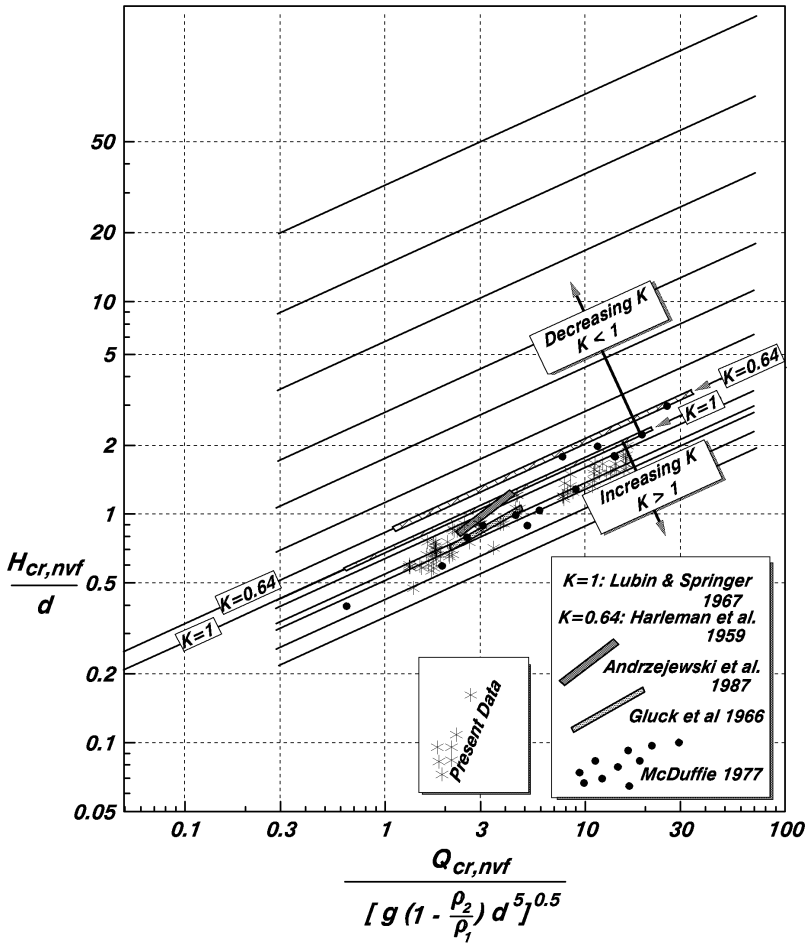

Figure 21: Discrepancies in published literature on $H_{cr,nvf}$ can be explained in terms of K

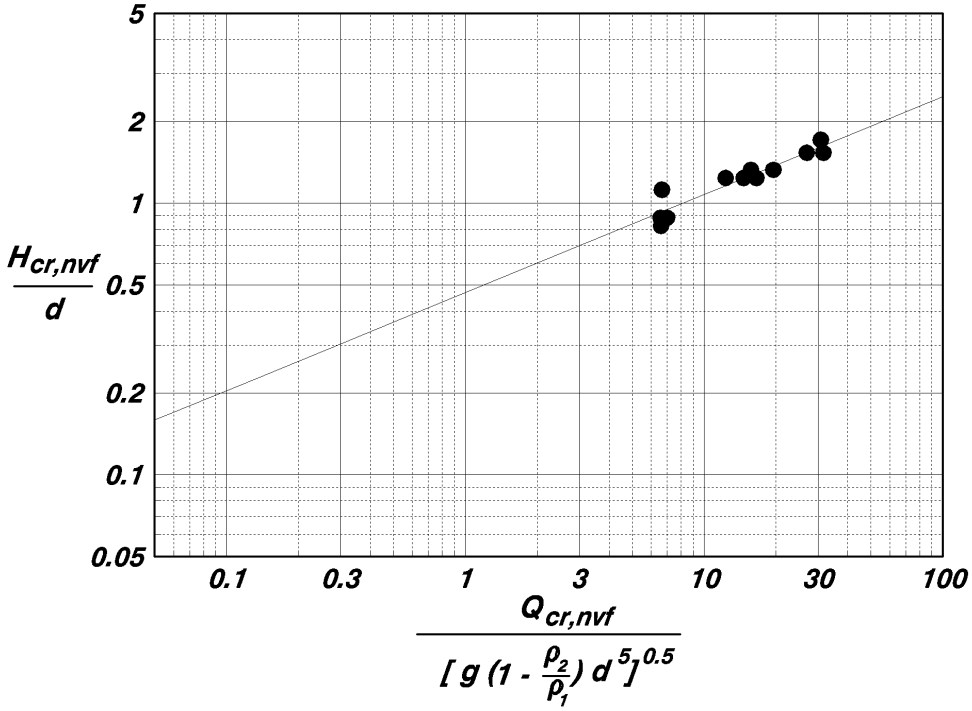

Figure 22: Measurements proved the validity of Eq. (4), *i.e.*, μ_2/μ_1 is less important than ρ_2/ρ_1

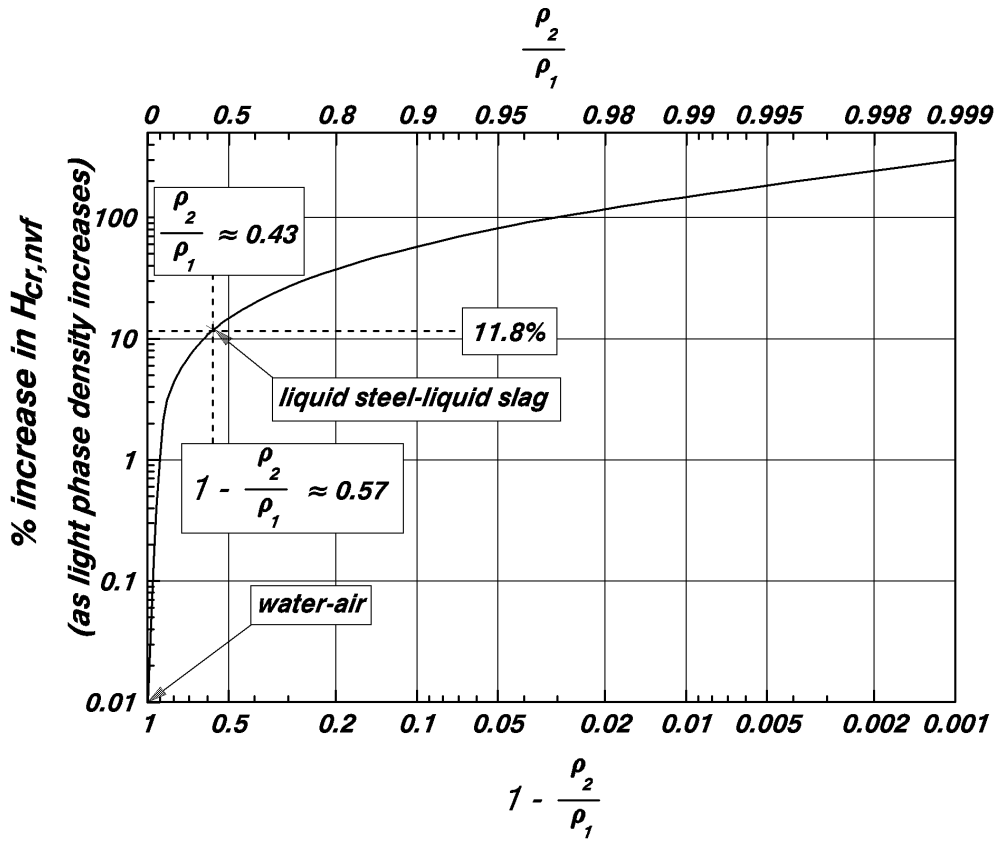

Figure 23: Relative density of the supernatant fluid and its influence on $H_{cr,nvf/d}$

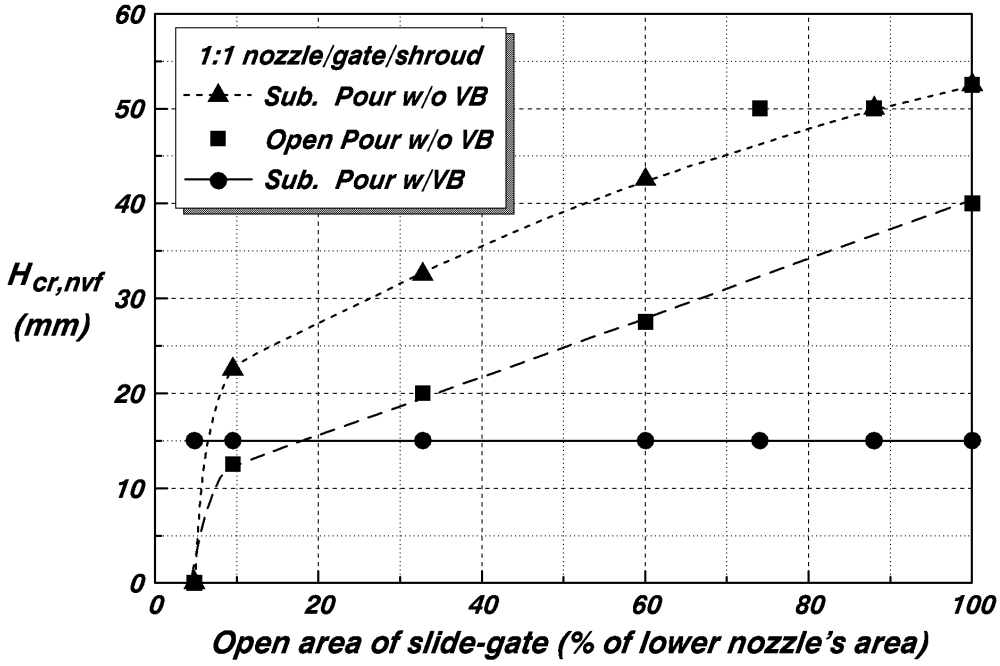

Figure 24: $H_{cr,nvf}$ varied with slide gate position (1:1 nozzle/slide-gate/shroud in 495mm ladle)

Table 1: Details of vortexing funnel *scale-up* experiments

Ladle Diameter D mm	Nozzle Diameter d mm	Nozzle Length l mm	Initial height of water, H_i mm	Geometric Scale Factor
495	15.3	53	425 ± 5	0.427
1160	35.6	123.5	995 ± 5	

Table 2: Density and viscosity of selected carbon steels and steelmaking slags[*]

wt% C in steel	Density at 50°C superheat	Viscosity at 50°C superheat
0.054 to 0.61	7000 to 7033 kg/m^3	0.065 to 0.07 Poise
%CaO-Al_2O_3-SiO_2 in slag	**Slag density at 1500°C**	**Slag viscosity at 1500°C**
50-05-45	2.62	3.5 Poise
40-20-40	2.61	3 Poise
34-30-36	2.78	12 Poise
30-10-60	2.44	35 Poise
25-10-65	2.32	100 Poise

[*] Source: Making Shaping and Treating of Steels, Ed. 11, Steelmaking and Refining Volume, 1998

Table 3: Range of density and viscosity ratios in non-Vortexing Funnel Trials[29]

Primary liquid-Lighter liquid	Density Ratio, ρ_2/ρ_1	Viscosity Ratio, μ_2/μ_1
Water-Cutting oil	0.83	45
Water-Dow 50®	0.96	48
Water-Texaco 1	0.93	2495
Water-Shell 1	0.9	547
Water-Dow 1000®	0.971	841
Water-Shell 2	0.87	1610
Water-Texaco 2	0.91	2967
Water-Dow 12500®	0.976	10555
$ZnCl_2$-Shell 1	0.529	36.5
$ZnCl_2$-Shell 2	0.511	123
$ZnCl_2$-Texaco 1	0.547	192
$ZnCl_2$-Texaco 2	0.535	228

Table 4: Details of non-vortexing funnel experiments to prove the lack of dependence of $H_{cr,nvf}$ on μ_2/μ_1 (see Table 3 for range of viscosities studied)

Ladle diameter, D mm	Nozzle diameter, d mm	Nozzle length, l mm
245	16.5	885